Center for Modeling of Turbulence and Transition
Research Briefs - 1991

Lumley's Energy Cascade Dissipation Rate Model for Boundary-Free Turbulent Shear Flows

B. S. Duncan

1. Motivation and Objective

True dissipation occurs mainly at the highest wavenumbers where the eddy sizes are comparatively small. These high wave numbers receive their energy through the spectral cascade of energy starting with the largest eddies spilling energy into the smaller eddies, passing through each wavenumber until it is dissipated at the microscopic scale. However, a small percentage of the energy does not spill continuously through the cascade but is instantly passed to the higher wave numbers[1]. Consequently, the smallest eddies receive a certain amount of energy almost immediately. As the spectral energy cascade continues, the highest wave number needs a certain time to receive all the energy which has been transferred from the largest eddies. As such, there is a time delay, of the order τ, between the generation of energy by the largest eddies and the eventual dissipation of this energy.

For equilibrium turbulence at high Reynolds numbers, there is a wide range where energy is neither produced by the large eddies nor dissipated by viscosity, but is conserved and passed from wavenumber to higher wavenumber. The rate at which energy cascades from one wavenumber to another is proportional to the energy contained within that wave number. This rate is constant and has been used in the past as a dissipation rate of turbulent kinetic energy. However, this is true only in steady, equilibrium turbulence. Most dissipation models contend that the production of dissipation is proportional the production of energy and that the destruction of dissipation is proportional to the destruction of energy. In essence, these models state that the change in the dissipation rate is proportional to the change in the kinetic energy. This assumption is obviously incorrect for the case where there is no production of turbulent energy, yet energy continues to cascade from large to small eddies. If the time lag between the onset on the energy cascade to the destruction of energy at the microscale can be modeled, then there will be a better representation of the dissipation process. Development of an energy cascade time scale equation will be discussed in Section 2.2.

2. Work Accomplished

2.1 Mean Flow Equations

For incompressible flow, the equations for continuity of mass and axial momentum are written as

$$\frac{\partial U_i}{\partial x_i} = 0$$

and

$$\frac{DU_i}{Dt} = \frac{\partial}{\partial x_j}\left(\nu\frac{\partial U_i}{\partial x_j} + \overline{u_i u_j}\right) - \frac{1}{\rho}\frac{\partial P}{\partial x_i}$$

where, $\overline{u_i u_j}$ is the turbulent Reynolds stress tensor. Using the eddy viscosity concept[2], the Reynolds stress may be related to the mean strain rate and a turbulent eddy viscosity,

$$-\overline{u_i u_j} = \nu_t \left(\frac{\partial U_i}{\partial x_j} + \frac{\partial U_i}{\partial x_j} \right) - \frac{2}{3} k \delta_{ij}. \tag{1}$$

The turbulent viscosity given in the above equation can be interpreted as a measure of the turbulent kinetic energy existing in the flow times a local length scale,

$$\nu_t = c k^{\frac{1}{2}} l$$

where c is an arbitrary constant. The definition used for this length scale is the primary discriminating factor between turbulence models and determines the number of equations which need to be solved. The length scale can be written in terms of the turbulent kinetic energy,k, and its dissipation rate,ϵ,

$$l = \frac{k^{\frac{3}{2}}}{\epsilon}.$$

Now, the momentum equation can be written as

$$\frac{DU_i}{Dt} = \frac{\partial}{\partial x_j} \left((\nu + \nu_t) \frac{\partial U_i}{\partial x_j} \right) - \frac{1}{\rho} \frac{\partial P}{\partial x_i}$$

where,

$$\nu_t = \frac{c_\mu k^2}{\epsilon} \tag{2}$$

and c_μ is a constant. The k and ϵ are determined by solving transport equations for the turbulent kinetic energy and the dissipation. These equations and the modification to the "standard" dissipation equation will be discussed in Section 2.2.

2.2 Turbulence Equations

Taking the Navier-Stokes equations and multiplying by $\hat{u}_i = U_i + u_i$ and then taking the time average yields an equation that contains both the energy equation for the mean velocity, U_i, and a mean energy equation for the fluctuating component of velocity,u_i. Eliminating the energy equation for the mean velocity yields the turbulent energy budget in the absence of a pressure gradient field[3],

$$\frac{Dk}{Dt} = -\frac{\partial}{\partial x_j} \left(\frac{1}{2} \overline{u_i u_i u_j} - 2\nu \overline{u_i s_{ij}} \right) - \overline{u_i u_j} S_{ij} - 2\nu \overline{s_{ij} s_{ij}}. \tag{3}$$

The last term in equation (3) is the rate at which viscous forces perform deformation work to the fluctuating strain rate, defined as

$$s_{ij} = \frac{1}{2} \left(\frac{\partial u_j}{\partial x_i} + \frac{\partial u_i}{\partial x_j} \right).$$

This term is the true viscous dissipation rate which drains kinetic energy from the system, $\epsilon = 2\nu s_{ij} s_{ij}$. This dissipation rate is important to the overall turbulence structure. The next to the last term in equation (3) serves to transport kinetic energy between the mean flow and the turbulence. It is generally referred to as the kinetic energy production term. Writing the mean strain, S_{ij}, as

$$S_{ij} = \frac{1}{2}\left(\frac{\partial U_j}{\partial x_i} + \frac{\partial U_i}{\partial x_j}\right)$$

the production term for incompressible flow is defined as

$$P_k = -\overline{u_i u_j} S_{ij} = \nu_t \left(\frac{\partial U_j}{\partial xi} + \frac{\partial U_i}{\partial x_j}\right)\frac{\partial U_i}{\partial x_j} \tag{4}$$

The last set of terms to be modeled represents the energy redistribution by viscous forces and are contained within the parenthesis on the right hand side of equation (3). From the definition of the fluctuating strain rate,

$$2\nu\overline{u_i s_{ij}} = \nu\frac{\partial k}{\partial x_j}$$

and using a mean gradient hypothesis, the triple correlation can be rewritten as

$$-\overline{u_i u_i u_j} = \frac{\nu_t}{\sigma_k}\frac{\partial k}{\partial x_j}$$

where σ_k is a constant of the order one. Combining all these modeling assumptions yields the high Reynolds number form of the turbulent kinetic equation,

$$\frac{Dk}{Dt} = \frac{\partial}{\partial x_j}\left(\left(\nu + \frac{\nu_t}{\sigma_k}\right)\frac{\partial k}{\partial x_j}\right) + \nu_t\left(\frac{\partial U_i}{\partial x_j} + \frac{\partial U_j}{\partial x_i}\right)\frac{\partial U_i}{\partial x_j} - \epsilon.$$

An equation of the following form has been widely used for modeling of the dissipation,

$$\frac{D\epsilon}{Dt} = \frac{\partial}{\partial x_j}\left(\left(\nu + \frac{\nu_t}{\sigma_\epsilon}\right)\frac{\partial \epsilon}{\partial x_j}\right) + P_\epsilon - \frac{1}{c}\frac{\epsilon^2}{k}.$$

The production term, P_ϵ has been assumed to be proportional to the turbulent kinetic energy production term, equation (4). This approximation places a direct correlation between the production of turbulent energy and the production of dissipation. Although this may be true at equilibrium, where by definition the dissipation equals the turbulent energy production, there are some deficiencies in this statement for the more general case. According to Lumley[1], the modeled dissipation rate equation should be written as,

$$\frac{D\epsilon}{Dt} = \frac{\partial}{\partial x_j}\left(\left(\nu + \frac{\nu_t}{\sigma_\epsilon}\right)\frac{\partial \epsilon}{\partial x_j}\right) + \frac{c_A}{c_D}\epsilon\mathcal{S} - \frac{1}{c_D}\frac{\epsilon^2}{k}. \tag{5}$$

The production term, P_ϵ, now represents the rate at which energy arrives at the dissipative wavenumbers through the energy cascade starting with low wavenumbers. In equation (5), $1/\mathcal{S}$ represents the characteristic time for energy to be transported to the dissipative wave numbers.

In the following equation, the term on the left hand side and the first term on the right represent the transport of the inverse time scale by advection and diffusion, respectively. The remaining terms are the production from the mean straining forces within the large scale mean flow structures and the dissipative losses at the microscale,

$$\frac{D\mathcal{S}}{Dt} = \frac{\partial}{\partial x_j}\left(\left(\nu + \frac{\nu_t}{\sigma_\mathcal{S}}\right)\frac{\partial \mathcal{S}}{\partial x_j}\right) + \left(\sqrt{S_{ij}S_{ij}} - \mathcal{S}\right)\frac{1}{c_b T}$$

The production and loss terms have been scaled by a characteristic time, T, which in this study has been taken to be a weighted function of the time scale for the large eddies, τ,

$$T = \frac{\tau}{2C_B}.$$

Since most energy enters the cascade at scales comparable to the integral scale, l, the characteristic time scale of the large eddies dictates the rate of energy transfer and is defined as $\tau = \frac{l}{u}$ for nearly isotropic turbulence. Using the approximation for the integral length scale as, $l = \frac{u^3}{\epsilon}$, the time scale becomes

$$\tau = 2\frac{k}{\epsilon}$$

which is valid even in nonequilibrium flows. Letting C_B be a function of mean and turbulent quantities, the inverse time scale equation can be written as

$$\frac{D\mathcal{S}}{Dt} = \frac{\partial}{\partial x_j}\left(\left(\nu + \frac{\nu_t}{\sigma_\mathcal{S}}\right)\frac{\partial \mathcal{S}}{\partial x_j}\right) + \frac{C_B}{c_B}\left(\sqrt{S_{ij}S_{ij}} - \mathcal{S}\right)\frac{\epsilon}{k}$$

where

$$C_B = 1 + \frac{9k\sqrt{S_{ij}S_{ij}}}{\epsilon}.$$

Determination of the modeling constants is discussed in the next section.

2.3 Model Constants

In this paper, only high Reynolds number turbulence has been considered. The model constants are examined for the grid turbulence case where the mean velocity gradients and strain rates vanish. For this case, turbulent intensity decays with the following proportionality,

$$\left(\frac{k}{k_0}\right) \propto \left(\frac{t}{t_0}\right)^{-n}, \text{ where, } t = \frac{x}{U_0}$$

so that the dissipation rate must decay as

$$\left(\frac{\epsilon}{\epsilon_0}\right) \propto \left(\frac{t}{t_0}\right)^{-(n+1)}.$$

Here, n is the decay rate and is typically in the range $1.1 \leq n \leq 1.3$. Substituting these relationships into the inverse time scale equation yields

$$\frac{1}{S} dS = -\frac{nC_B}{tc_B} dt.$$

After integration, this equation is

$$S = \alpha t^{-\frac{nC_B}{c_B}}$$

where α is a constant of integration. For there to be an inverse scaling relationship between S and t, the exponent in the above equation must reduce to -1 for the grid turbulence case. Since the coefficient C_B reduces to 1.0 in grid turbulence, then

$$c_B = n.$$

In this study, n has been set to 1.1 and held constant[4], which sets the value of c_B. Now using the fact that, initially,

$$S_0 t_0 = \frac{3}{2\sqrt{2}}$$

the coefficients c_A and c_D are related as follows

$$\frac{1}{c_D} = \frac{3}{2\sqrt{2}} \frac{c_A}{c_D} + \frac{n+1}{n}.$$

The coefficient c_μ has been evaluated for equilibrium turbulence where, where $P_k = \epsilon$. Rewriting equation (2) as

$$c_\mu = \frac{\nu_t \epsilon}{k^2}$$

and using equations (1) and (4), this coefficients is

$$c_\mu = \frac{\overline{u_i u_j}^2}{k^2} = 0.09.$$

After the above analysis, the only adjustable parameters are $\frac{c_A}{c_D}$ and the σ coefficients, which should be of the order one. The complete set of optimized coefficients is given in Table 1.

$\sigma_k = 0.9$	$n = 1.1$
$\sigma_\epsilon = 1.1$	$c_B = n$
$\sigma_S = 1.0$	$C_B = 1 + \frac{9k\sqrt{S_{ij}S_{ij}}}{\epsilon}$
$c_\mu = 0.09$	$\frac{1}{c_D} = \frac{3}{2\sqrt{2}} \frac{c_A}{c_D} + \frac{n+1}{n}$
$\frac{c_A}{c_D} = 1.13$	

Table 1. k–ϵ–S Model Coefficients

2.4 Free Shear Flows

The three turbulent transport equations are solved implicitly using the finite difference technique of Spalding[5] for parabolic equation systems. An initial profile is imposed upon the first marching plane for the turbulent kinetic energy and the dissipation, and $\mathcal{S}$ is initially set to $\mathcal{S}_i = \frac{\epsilon_0}{k_0}$. In the mixing layer and jet cases, the initial plane was equally divided into a uniform velocity field and still air. For the case of the plane wake, this initial profile came from a flat plate calculation computed with the same solution technique. Starting with the initial plane, the flow field is developed by marching the transport equations downstream and applying the following boundary conditions,

Planar Jet

Centerline ($y = 0$) $\quad \frac{\partial k}{\partial y} = 0 \ , \ \frac{\partial \epsilon}{\partial y} = 0$

$$\mathcal{S}_{y=0} = \frac{\mathcal{S}_{old} c_b k U_{y=0} + \frac{\partial}{\partial y}\left((\nu+\nu_t)\frac{\partial \mathcal{S}}{\partial y}\right)}{c_b k U_{y=0} + \epsilon \Delta x}$$

Far Field ($y = y_{max}$) $k = 0 \ , \ \epsilon = 0 \ , \ \mathcal{S} = 0$

Round Jet

Centerline ($r = 0$) $\quad \frac{\partial k}{\partial r} = 0 \ , \ \frac{\partial \epsilon}{\partial r} = 0$

$$\mathcal{S}_{r=0} = \frac{\mathcal{S}_{old} c_b k U_{r=0} + \frac{\partial}{\partial r}\left((\nu+\nu_t)\frac{\partial \mathcal{S}}{\partial r}\right)}{c_b k U_{r=0} + \epsilon \Delta x}$$

Far Field ($r = r_{max}$) $k = 0 \ , \ \epsilon = 0 \ , \ \mathcal{S} = 0$

Planar Mixing Layer

Centerline ($y = y_{min}$) $\frac{k}{U^2_{y=ymin}} = 0.015, \frac{\epsilon L}{U^3_{y=ymin}} = 3.5 \times 10^{-6}$

$$\mathcal{S}_{y=ymin} = \frac{\epsilon}{k}$$

Far Field ($y = y_{max}$) $k = 0 \ , \ \epsilon = 0 \ , \ \mathcal{S} = 0$

Planar Wake

Centerline ($y = 0$) $\quad \frac{\partial k}{\partial y} = 0 \ , \ \frac{\partial \epsilon}{\partial y} = 0$

$$\mathcal{S}_{y=0} = \frac{\mathcal{S}_{old} c_b k U_{y=0} + \frac{\partial}{\partial y}\left((\nu+\nu_t)\frac{\partial \mathcal{S}}{\partial y}\right)}{c_b k U_{y=0} + \epsilon \Delta x}$$

Far Field ($y = y_{max}$) $k = 0 \ , \ \epsilon = 0 \ , \ \mathcal{S} = 0$

The solutions have been checked after several hundred steps to insure that the profiles have become self-similar.

2.4.1 Planar Jet

The three equation k–ϵ–S model performed very well for planar jet flow when compared to the experimental data of Gutman and Wygnanski[6], Bradbury[7] and Heskestad[8]. Mean velocities profiles given in Figure 1 are well predicted by both the k–ϵ–S model and the standard k–ϵ model, which is reassuring since the coefficients for both of these models were optimized for the planar jet case. The spreading rates predicted by both models are within the experimental range and are given in Table 2.

There is a slight discrepancy between the k–ϵ–S model and the standard k–ϵ model for centerline kinetic energy as can be seen in Figure 2. However, both predictions are well within the range of experimental measurements, which show a considerable spread near the centerline of the jet. Both predictions are closely aligned with the data of Bradbury[7].

Shear stress is also well predicted (see Figure 3) where the standard k–ϵ model over-predicts the shear stress at the edge of the jet in comparison to the data of Gutman and Wynanski[6] and Bradbury[7]. The k–ϵ–S model predicts a narrower profile, also indicated by the smaller spreading rate, which agrees with Bradbury's measurements. Towards the centerline of the jet, both models accurately predict the increase in shear stress and the extrema near $\frac{y}{x} = 0.08$.

For the next two figures, Figures 4 and 5, there is no experimental data available for comparison. The dissipation reaches a maximum at the location of the peak shear stress, Figure 4. From this extrema, the dissipation decreases toward the centerline and also eventually trails off to zero at the edge of the jet. Figure 5 shows the behavior of the time scale for the planar jet. Notice that the minimum energy transfer time between the large scale structure to the dissipative microscale is in the middle of the jet (where $\mathcal{S}$ is a maximum since the dimension of $\mathcal{S}$ is t^{-1}).

2.4.2 Axisymmetric Jet

A primary problem with the standard k–ϵ model is its predictive capability for a 2–D versus a 3–D jet, the free jet anomaly. In Figures 6 – 10, the standard k–ϵ model is unable to predict any of the turbulence quantities correctly, overpredicting not only the turbulent kinetic energy and the shear stress but also the mean velocity. The standard k–ϵ can be "fixed" using a suggestion by Pope[9]. Writing the standard ϵ equation for reference,

$$\frac{D\epsilon}{Dt} = \frac{\partial}{\partial x_j}\left(\left(\nu + \frac{\nu_t}{\sigma_\epsilon}\right)\frac{\partial \epsilon}{\partial x_j}\right) + c_1 P_k \frac{\epsilon}{k} - \frac{1}{c}\frac{\epsilon^2}{k}$$

the correct spreading rate can be obtained by changing c_1 from its standard value of 1.45 to 1.6 (see Table 2). Clearly, by modifying a coefficient, the standard k–ϵ model is capable of predicting the correct spreading rate; however, this model cannot be considered general. The spreading rate predicted by the k–ϵ–S model is very close to the experimentally measured rate and has been obtained with no modifications to the model.

Comparisons between the k–ϵ–S model and the experimental data[10,11,12], Figures 6 – 10, indicates that the new model accurately predicts the mean velocity profiles and the shearing stress across the jet. Less accurately predicted by the k–ϵ–S model is the centerline turbulent kinetic energy, Figure 7, where there is considerable scatter in the experimental data.

2.4.3 Planar Mixing Layer

For the case of a planar mixing layer, neither model accurately predicts the high speed side of the layer (see Figures 11 – 15). The experimental data[13] contains a much more dispersive edge compared to the computations, Figure 11. One explanation may be wind tunnel noise. Adding a boundary condition specifying a given noise level, 12 percent fluctuating velocity, increases the spreading on the high speed side of the computations and improves the comparisons with the data. This boundary condition is used with both models. Unfortunately, there is no way

to determine what the true noise level was in the experiments or whether its effect has been properly accounted for computationally.

An analytical solution for the mean velocity profile has been described by Schlichting[14]. This analytic solution lies between the experimental data and the two computational models for the case when $\sigma = 9.5$ (σ is a "tweeking" constant used to tune the analytic solution to match the experimental data. Typical values of σ are between 9[13] and 11[15].)

Both the k–ϵ–S and the standard k–ϵ model predict the peak value of turbulent kinetic energy quite well (Figure 12). However, this peak is shifted toward the low speed side of the mixing layer compared to the experimental peak. Patel[16] indicated that the data of Wygnanski and Fielder[13] had shifted towards the low speed side, which is opposite from the trend noticed in this study. Since the discrepancy between the data and the computations lies on the high speed side of the mixing layer, the problem could be a result of wind tunnel noise as previously mentioned. In the the plot of Reynolds stresses, Figure 13, both models over predict the shear stress by nearly 30 percent and consequently over-predict the spreading rate given in Table 2.

The k–ϵ–S model and the standard k–ϵ model predict almost identical levels of dissipation (Figure 14). Since a turbulent kinetic energy level is specified at the high speed boundary, the dissipation is also specified on this boundary. A constant value of $\frac{\epsilon L}{U^3_{max}} = 6.5 \times 10^{-6}$ gave the best fit to the data. Figure 15 shows the inverse time scale distribution through the mixing layer. The minimum energy transfer time, where $\mathcal{S}$ is a maximum, corresponds to the location of the maximum shear stress. At the high speed edge of the mixing layer, the time scale is specified to be $\mathcal{S} = \frac{\epsilon}{k}$.

2.4.4 Planar Wake

For the case of the planar wake, the mean velocity profile is correctly predicted towards the centerline of the wake, but drops off too quickly at the wake edges (see Figure 16). Although the mean velocity shows the correct shape in Figure 16, the centerline velocity is high compared to the analytical solution described in Reference [14] (see Figure 17). As a result, the spreading rates, $(\frac{U_\infty}{U_\infty - U_0}\frac{dy_{\frac{1}{2}}}{dx})$, predicted by the turbulence models are 6 percent too low for the k–ϵ–S model and 3 percent too low for the k–ϵ model as compared to the analytical solution. In other words, the turbulence models are predicting a much more compact wake with a smaller velocity defect than is seen in the experimental data or the analytical fit. This trend is also seen in the turbulent kinetic energy profiles in Figure 18 where the k–ϵ–S model can predict the correct maximum intensity but drops off too quickly towards the edges. Also, although the computed peak value for shear stress is correct the width of the curve is too narrow, with the location of the extrema lying too near the centerline (see Figure 19).

The dissipation levels computed by the models apparently reduce the turbulent intensity of the flow too much near the edges of the wake, which prevents the wake from spreading. There is unfortunately no experimental data to compare with the dissipation curves in Figure 20. Interestingly, the location of the minimum energy

transfer time in Figure 21 is towards the outer edges of the wake where the mean flow should exert its greatest influence.

	Experiment	k–ϵ–$\mathcal{S}$ Model	k–ϵ Model
Planar Jet	0.11–0.12	0.114	0.114
Round Jet	0.085–0.095	0.095	0.126, $c_1 = 1.45$ 0.0928, $c_1 = 1.6$
Planar Mixing Layer	0.16	0.186	0.186
Planar Wake	.101[14]	0.095	0.098

Table 2. Spreading Rate Comparisons for Free Shear Flow

3. Future Work

Future plans include:

i) Extending this model to wall bounded flow. Specifically, a low Reynolds number version of this model will be developed for near wall turbulence.

ii) Continuing to run this model for more test cases over a variety of flow fields.

4. References

[1] Lumley, J. L., "Some comments on turbulence", Physics of Fluids 4 (1992).

[2] Boussinesq, J., "Essai sur la théorie des eaux courantes", Mém. prés. Acad. Sci. **XXIII** (46) (1877).

[3] Tennekes, H. & Lumley, J. L., *A First Course in Turbulence* The MIT Press (1972).

[4] Launder, B. E., "Turbulence transport models for numerical computation of complex turbulent flows",*Measurements and Predictions of Complex Turbulent Flows* Von Karman Institute for Fluid Dynamics, Rhode Saint Genese, Belgium (1980).

[5] Spalding,D. B., *GENMIX: A General Computer Program for Two-Dimensional Parabolic Phenomena* Pergamon Press (1977).

[6] Gutmark, E. & Wygnanski, I., "The Planar Turbulent Jet", Journal of Fluid Mechanics **73**, 465–495 (1976).

[7] Bradbury, L. J. S., "The Stucture of the Self-Preserving Jet" Journal of Fluid Mechanics **23** 31–64 (1965).

[8] Heskestad, G., "Hot-Wire Measurements in a Plane Turbulent Jet" Journal of Applied Mechanics (1965).

[9] Pope, S. B., "An Explanation of the Turbulent Round-Jet/Plane-Jet Anomaly" AIAA Journal **16** (1978).

[10] Wygnanski, I. & Fiedler, H. E., "Some measurements in the self-preserving jet" Journal of Fluid Mechanics **38** 577–612.

[11] Rodi, W., "A New Method of Analyzing hot-wire Signals in Highly Turbulent Flow and Its Evaluation in Round Jet" Disa Information No. 17 (1975).

[12] Abbiss, J. B. & Bradbury, L. J. S. & Wright, M. P., "Measurements in an Axisymmetric Jet Using a Photon Correlator" *Proceeding of LDA Symposium* Copenhagen (1975).

[13] Wygnanski, I. & Fiedler, H. E., "The two-dimensional mixing region", Journal of Fluid Mechanics **41** 327–361 (1970).

[14] Schlichting, H.,*Bounday-Layer Theory* McGraw-Hill (1951).

[15] Liepmann, H. W. & Laufer, J., "Investigations of Free Turbulent Mixing" NACA Technical Note 1257 (1947).

[16] Patel, R, "An Experimental Study of a Plane Mixing Layer", AIAA Journal **11** (1) (1973).

[17] Chevray, R. & Kovasznay, L. S. G., "Turbulence Measurements in the Wake of a Thin Flat Plate" AIAA Journal **7** (1969).

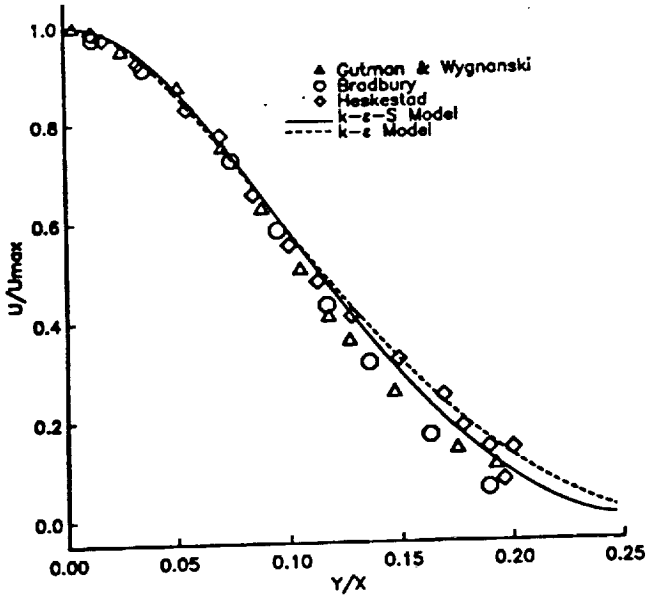

Figure 1: Mean velocity profile for a turbulent, planar jet. U_{max}: centerline velocity.

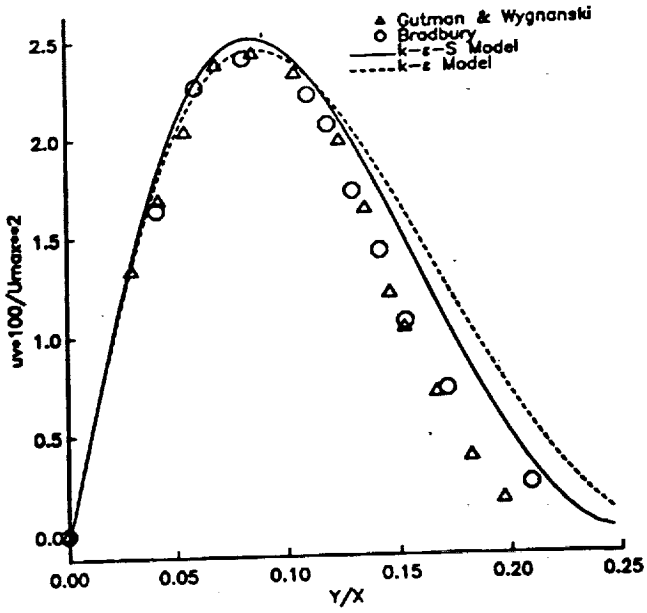

Figure 3: Shear stress profile for a planar jet. U_{max}: centerline velocity.

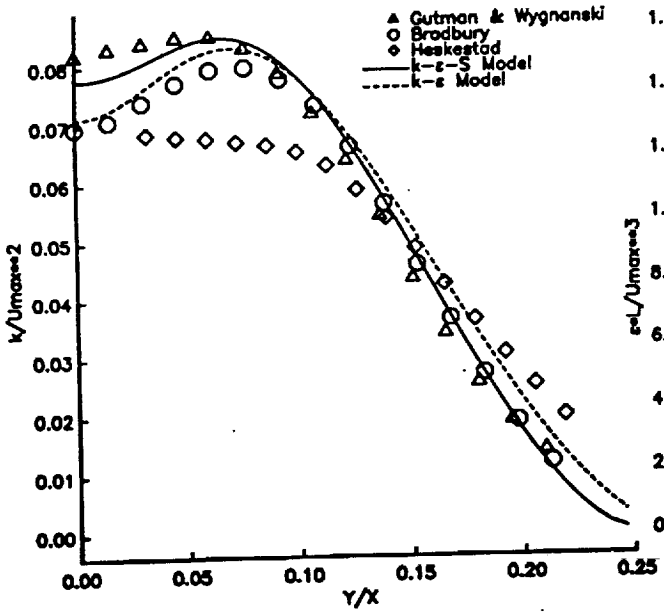

Figure 2: Turbulent kinetic energy profile for a planar jet. U_{max}: centerline velocity.

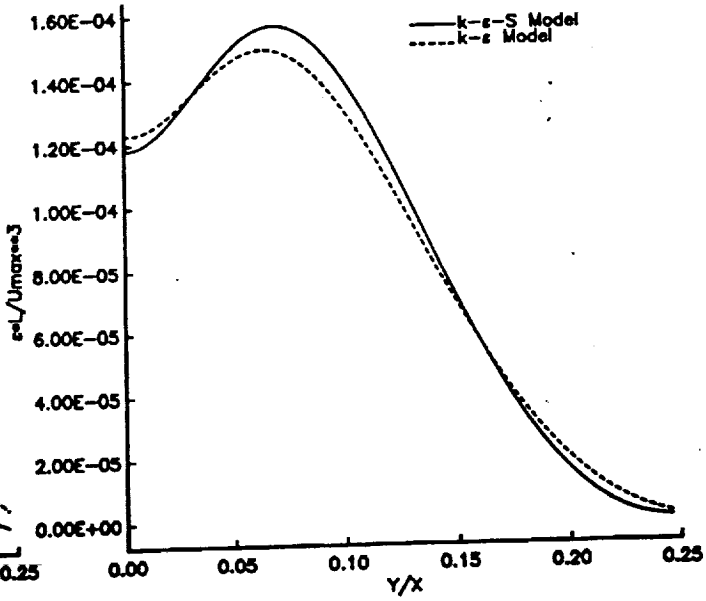

Figure 4: Dissipation rate profile for a planar jet. U_{max}: centerline velocity.

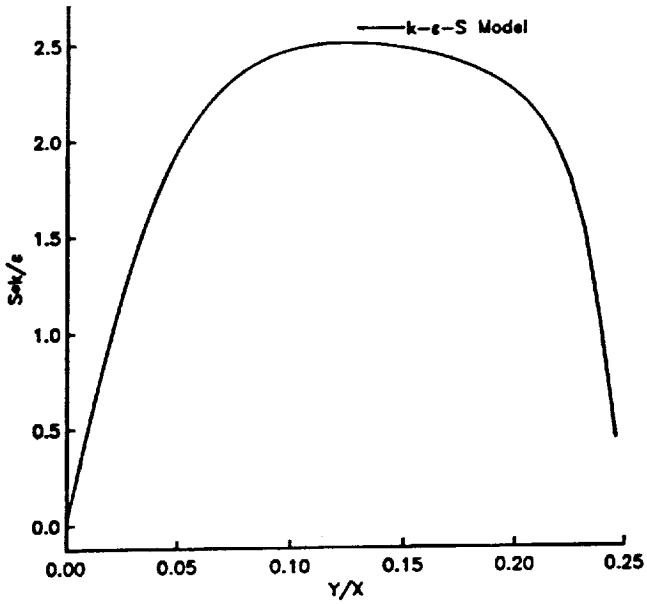

Figure 5: Time scale profile for a planar jet

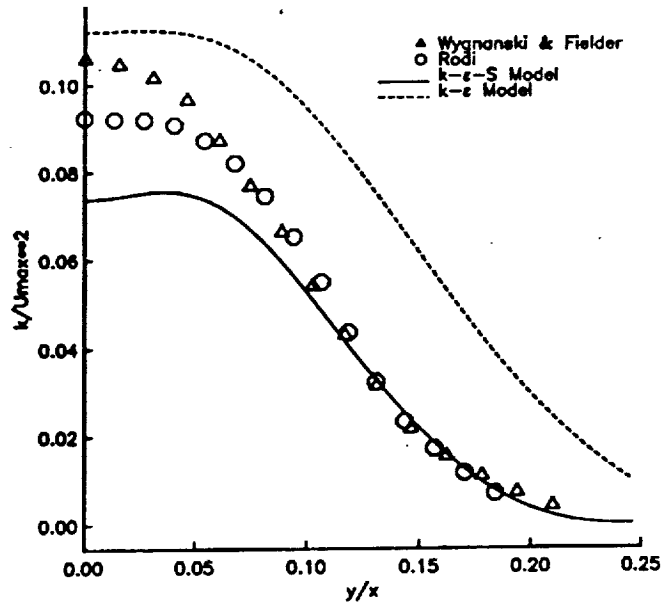

Figure 7: Turbulent kinetic energy profile for an axisymmetric jet. U_{max}: centerline velocity.

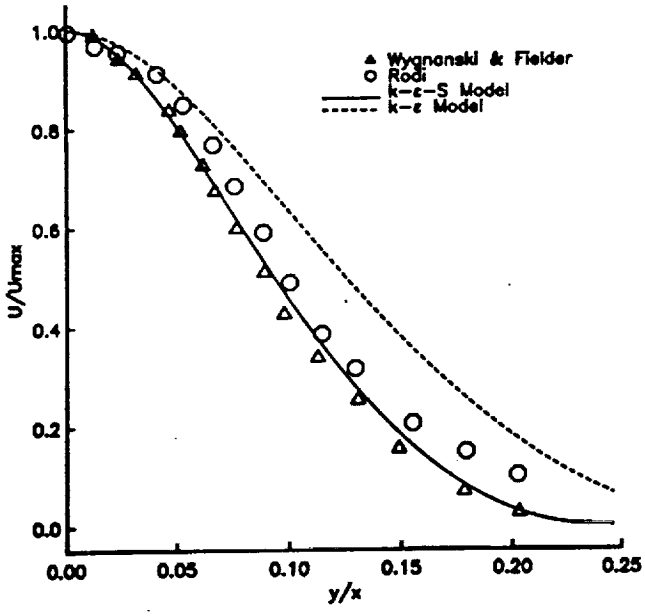

Figure 6: Mean velocity profile for a turbulent, axisymmetric jet. U_{max}: centerline velocity.

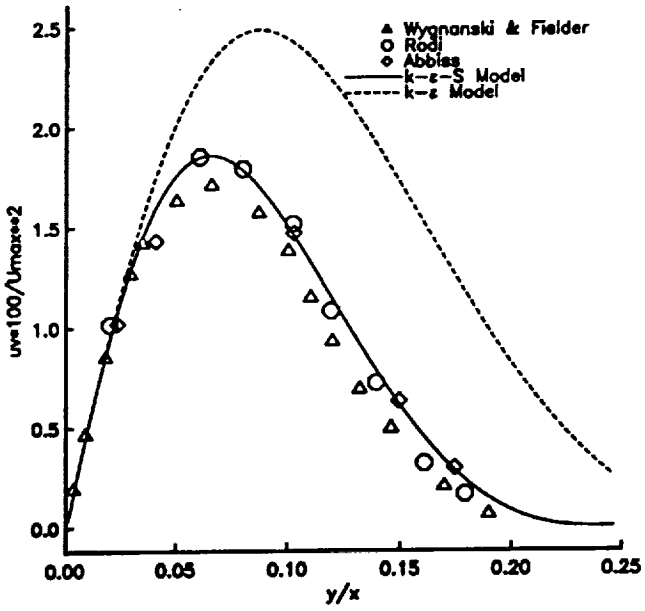

Figure 8: Shear stress profile for an axisymmetric jet. U_{max}: centerline velocity.

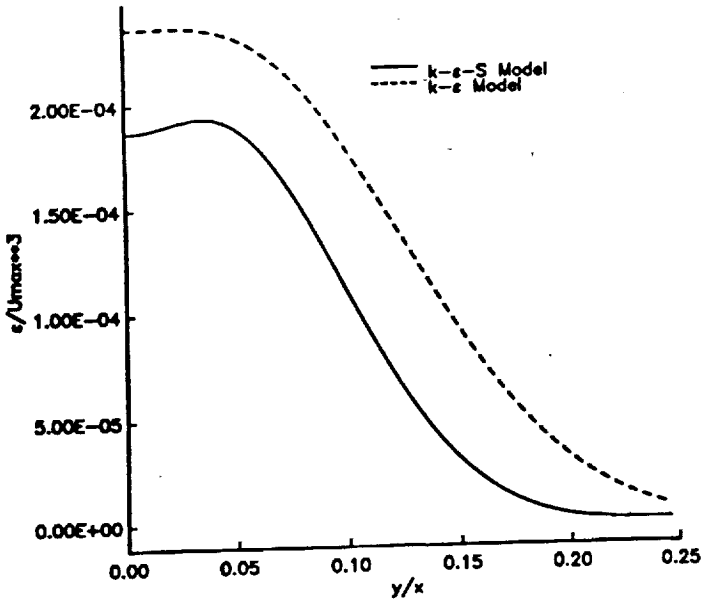

Figure 9: Dissipation rate profile for an axisymmetric jet. U_{max}: centerline velocity.

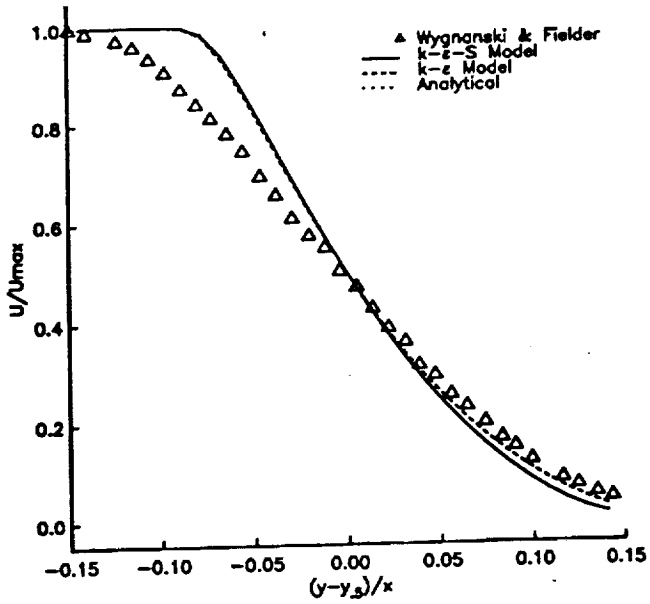

Figure 11: Mean velocity profile for a planar mixing layer. U_{max}: centerline velocity. — analytical solution

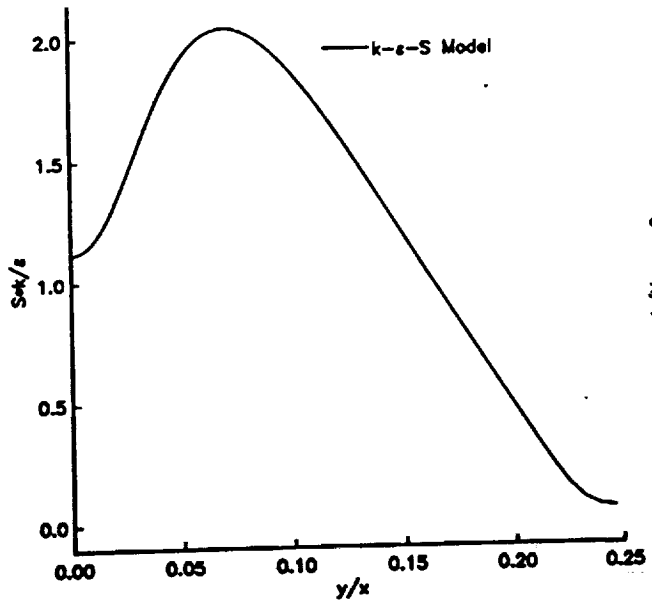

Figure 10: Time scale profile for an axisymmetric jet

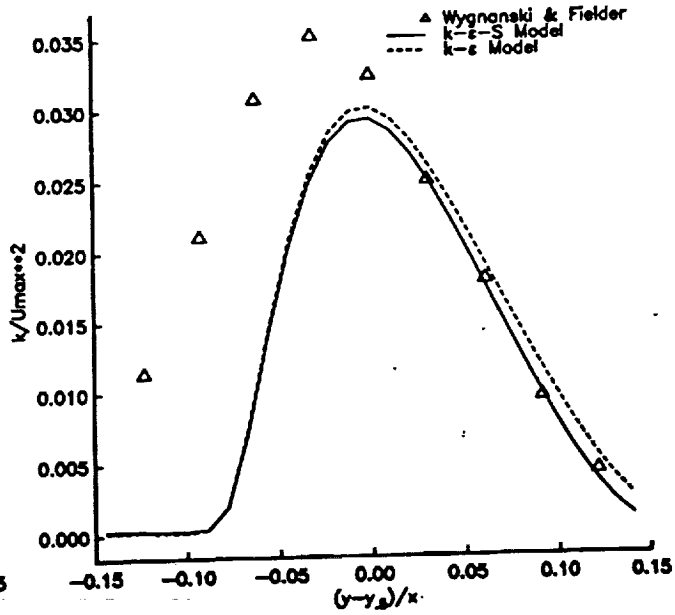

Figure 12: Turbulent kinetic energy profile for a planar mixing layer. U_{max}: centerline velocity.

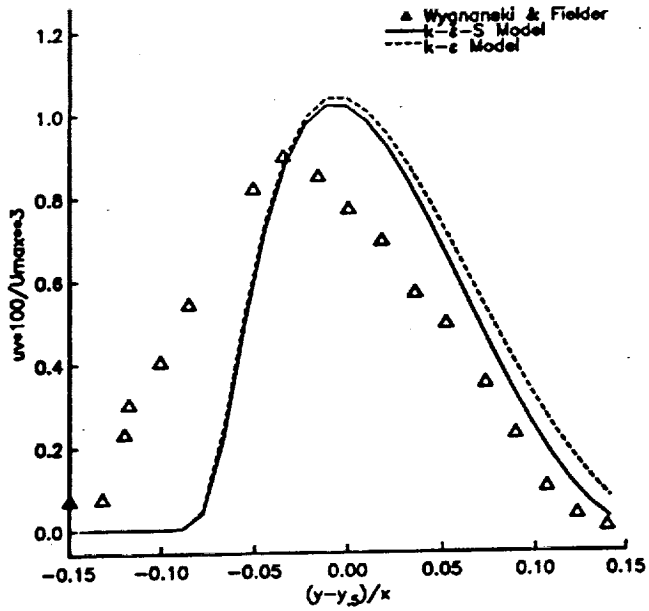

Figure 13: Shear stress profile for a planar mixing layer. U_{max}: centerline velocity.

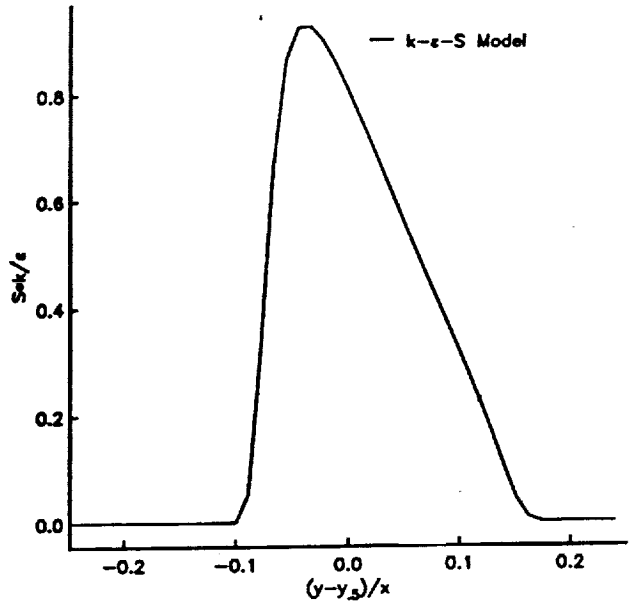

Figure 15: Time scale profile for a planar mixing layer

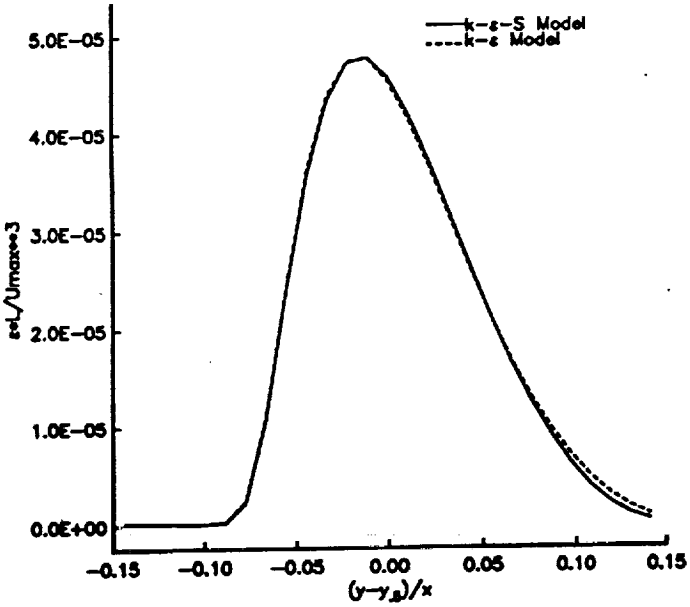

Figure 14: Dissipation rate profile for a planar mixing layer. U_{max}: centerline velocity.

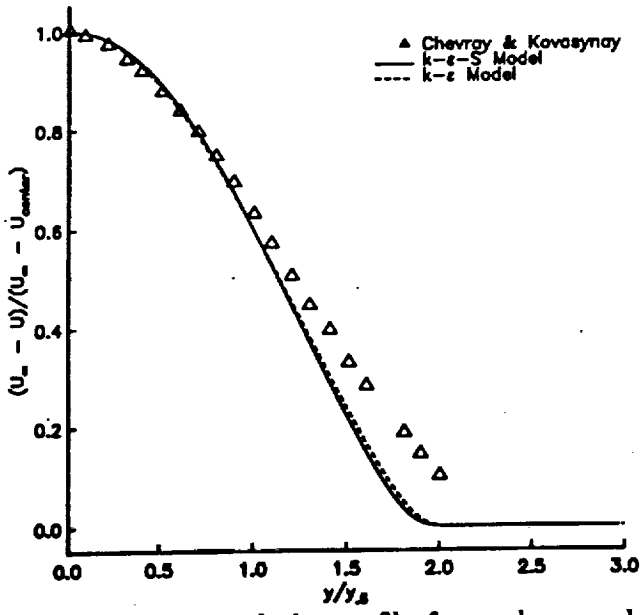

Figure 16: Mean velocity profile for a planar wake behind a flat plate. U_{center}: centerline velocity, U_{∞}: freestream velocity. — analytical solution

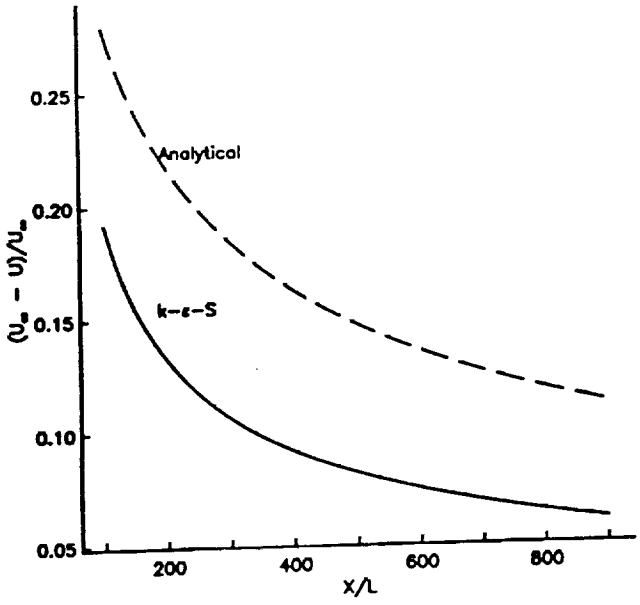

Figure 17: Axial mean centerline velocity for a planar wake behind a flat plate. U_∞: freestream velocity.

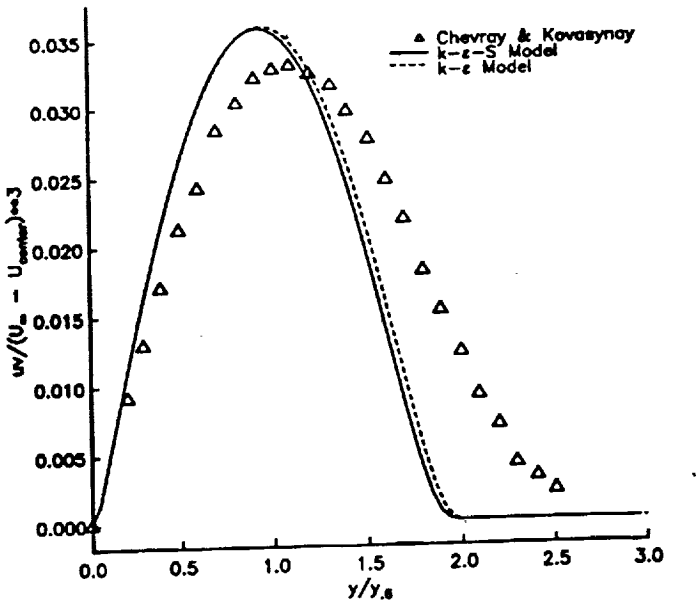

Figure 19: Shear stress profile for a planar wake behind a flat plate. U_{center}: centerline velocity, U_∞: freestream velocity.

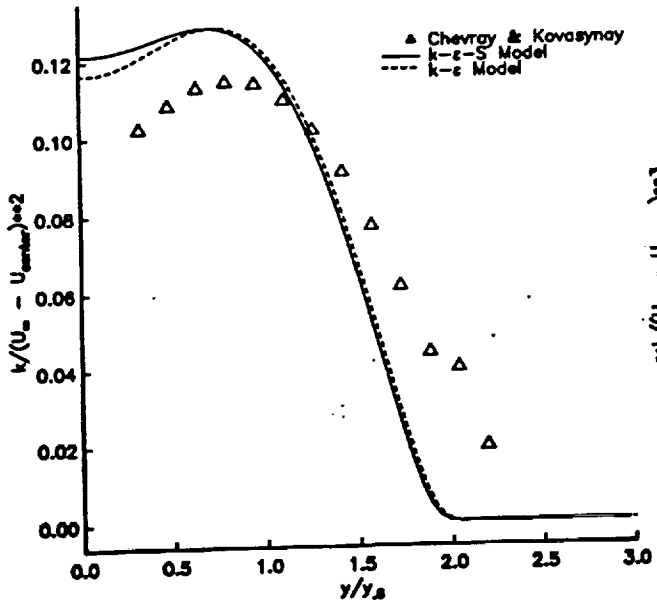

Figure 18: Turbulent kinetic energy profile for a planar wake behind a flat plate. U_{center}: centerline velocity, U_∞: freestream velocity.

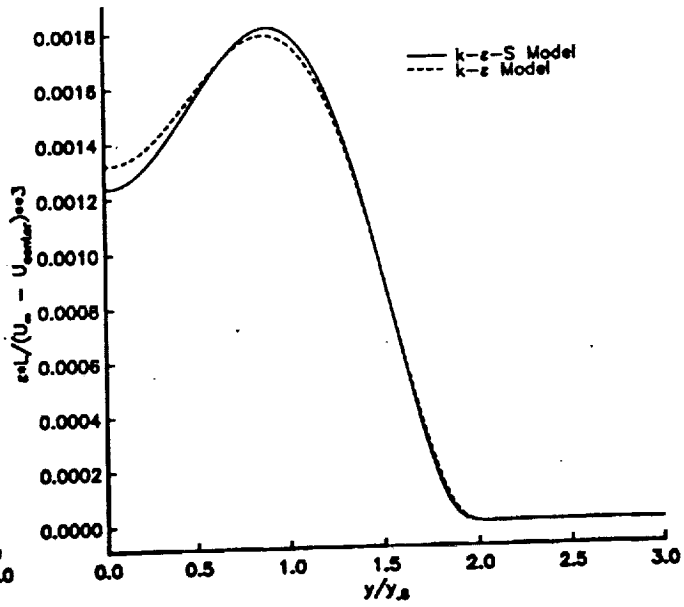

Figure 20: Dissipation rate profile for a planar wake behind a flat plate. U_{center}: centerline velocity, U_∞: freestream velocity.

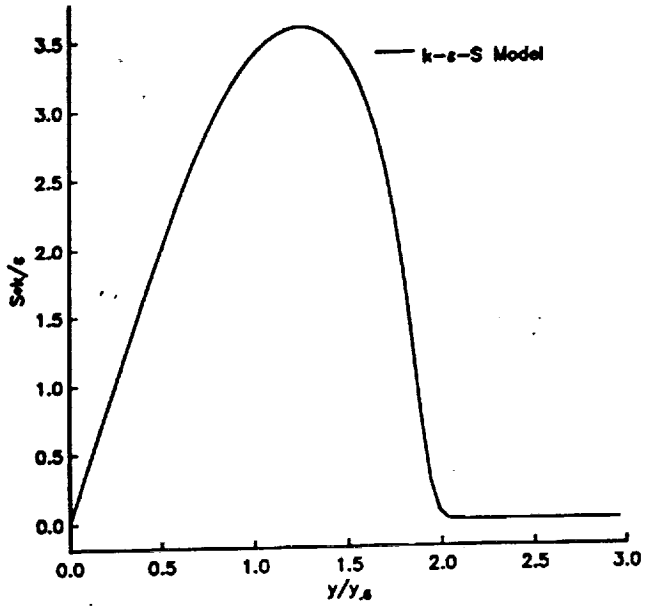

Figure 21: Time scale profile for a planar wake behind a flat plate